Arabian Journal of Chemistry (2022) **15**, 103968

King Saud University

Arabian Journal of Chemistry

www.ksu.edu.sa
www.sciencedirect.com

ORIGINAL ARTICLE

Comparative identification of the metabolites of dehydrocorydaline from rat plasma, bile, urine and feces by both the targeted and untargeted liquid chromatography/mass spectrometry strategies

Yueguang Mi [a,1], Xiangyang Wang [a,b,1], Meiting Jiang [a,1], Meiyu Liu [a], Xiaoyan Xu [a], Ying Hu [a], Hongda Wang [a], Feifei Yang [a], Jing Wang [c], Jie Liu [a], Qi Jing [a], Boxue Chen [a], Xue Li [a,*], Wenzhi Yang [a,*]

[a] *State Key Laboratory of Component-based Chinese Medicine, Tianjin University of Traditional Chinese Medicine, 10 Poyanghu Road, Jinghai, Tianjin 301617, China*
[b] *Tasly Academy, Tasly Holding Group Co., Ltd., Tianjin 300410, China*
[c] *Waters Technology Co., Ltd., 156 Jinghai Fourth Road, Beijing 101102, China*

Received 30 January 2022; accepted 16 May 2022
Available online 21 May 2022

KEYWORDS

Dehydrocorynine;
Precursor ions list;
Data-dependent acquisition;
Data-independent acquisition;
Mass defect filtering;
Metabolite characterization

Abstract Severe interference from the endogenous substances is often encountered in characterizing the drug metabolites by liquid chromatography/mass spectrometry using data-dependent acquisition (DDA). To add a precursor ions list (PIL) by DDA or apply data-independent acquisition (DIA) coupled with post-acquisition data processing (such as mass defect filtering, MDF) may assist to target more metabolites from the complex biosamples. Dehydrocorynine (DHC) is a bioactive alkaloid compound rich in *Corydalis yanhusuo*. We integrated both PIL-DDA and DIA-MDF strategies to probe the metabolites of DHC simultaneously from the rat plasma, bile, urine, and feces. Chromatographic separation was performed on an HSS C18 SB column. The positive-mode collision-induced dissociation-MS^2 data of DHC metabolites were recorded by PIL-DDA on both the QTrap 4500 and Vion IM-QTOF mass spectrometers, and by $HDMS^E$ on Vion IM-QTOF. Efficient workflows to process the high-definition DDA (HDDDA) and $HDMS^E$ data were elaborated. Totally 40 metabolites (orally administrated at the dose of 100 mg/kg) were identified or tentatively characterized, involving 30 from bile, 16 from feces, 7 from plasma, and 18 from urine.

* Corresponding authors.
E-mail addresses: tjdxsyx@163.com (X. Li), wzyang0504@tjutcm.edu.cn (W. Yang).
[1] These authors contributed equally to this work.

Peer review under responsibility of King Saud University.

Production and hosting by Elsevier

https://doi.org/10.1016/j.arabjc.2022.103968

The methoxyls and C-5/C-6/C-8 were the main sites prone to be metabolized via demethylation and oxidation, and further glucuronic acid conjugation and sulfuric acid conjugation. Compared with literature, we can newly discover 17 metabolites in bile, and, for the first time, report the metabolites of DHC from rat urine and feces. Conclusively, the presented PIL-DDA and DIA-MDF strategies are powerful in elucidating the drug metabolites, which thus provides reference to characterizing the metabolic profiles of traditional Chinese medicine components.

1. Introduction

Corydalis Rhizoma (Yan-Hu-Suo) is a well-known traditional Chinese medicine, prepared from the dry tuber of *Corydalis yanhusuo* W. T. Wang (Wang et al., 2016). The alkaloids in the *Corydalis* species are considered to be the main active ingredients for the treatment of diseases. Specifically, dehydrocorydaline (DHC) is an isoquinoline protoberberine alkaloid naturally occurring to *C. yanhusuo* with the molecular formula of $C_{22}H_{24}NO_4$ and the content of 1.24–3.24 mg/g (Wang et al., 2017a). DHC has shown various biological activities, such as the anti-inflammation (Kong et al., 2020), anti-depression (Jin et al., 2019), anti-tumor (Hu et al., 2019), analgesic effect (Xiao et al., 2019), and protective action on the cardiovascular system (Chen et al., 2020), and thus is used as a marker compound for the quality control of the herbal medicine Corydalis Rhizoma (Wang et al., 2017a; Zhang et al., 2020). Recently, a cross-mapping strategy involving multiple doses and samples by liquid chromatography/mass spectrometry (LC-MS) was reported, which could characterize up to 127 metabolites after oral administration of Corydalis Rhizoma at the clinical dose of 1.4 g/kg (Yu et al., 2021). Besides, an HPLC-ESI-QTrap-MS approach was developed to identify the metabolites of DHC in the rat plasma and bile after oral administration of DHC (97.5 mg/kg), by which 18 metabolites were identified from the bile and 9 ones in plasma (Guan et al., 2017). In general, *O*-demethylation, hydroxylation, dihydroxylation, glucuronidation of *O*-demethyl DHC, sulfation of *O*-demethyl DHC, and dihydroxylation of dehydro-DHC, were the main metabolic pathways for DHC. The pharmacokinetic profiles of DHC after oral administration of *C. yanhusuo* and pure DHC were compared, which exhibited the *C. yanhusuo* extract could accelerate the absorption of DHC and slow down its elimination (Li et al., 2014). To comprehensively identify the metabolites of DHC from various rat tissues (e.g., plasma, bile, urine, and feces) by advanced LC-MS strategy is crucial to investigate its potential in the development of new drug.

LC-MS has been extensively utilized to qualitatively and quantitatively analyze the metabolites of drugs and traditional Chinese medicine (TCM) components, because of its high sensitivity and versatile scan approaches (Kang et al., 2020; Luo and Xing, 2021; Zhang et al., 2017). In the case of MS scan method, data-dependent acquisition (DDA) is preferably applied (Yu et al., 2021), by which the recorded MS^2 or MS^n data can be directly analyzed based on the definite precursor-product ions information. However, severe interference from the endogenous substances is often encountered due to the relatively weak signal intensity for the drug metabolites, which can thus result in the low coverage of those interested components in acquiring their fragmentation information. Previous researches have demonstrated the addition of a table that contains the components of interest (dubbed the precursor ions list, PIL) can greatly improve the coverage of DDA in the untargeted characterization of the TCM components (Fu et al., 2019; Wang et al., 2021a; Wang et al., 2022). In contrast, data-independent acquisition (DIA), using MS^E (Li et al., 2021), $HDMS^E$ (Radchenko et al., 2020), or SWATH (Kang et al., 2020), is able to cover all the precursor ions thus achieving the highest coverage in the fragmentation information recording. In particular, the utilization of ion mobility-mass spectrometry (IM-MS) can better resolve the complicated peaks yielding the high-definition MS^1/MS^2 spectra, which is beneficial to the metabolites identification (Wang et al., 2021a; Wang et al., 2022). Moreover, PRM (parallel reaction monitoring) and *p*MRM/IDA-EPI (predictive multiple reaction monitoring-information dependent acquisition-enhanced product ion scan) are also powerful in identifying the metabolites for a pure compound or the complicated TCM extract (Dong et al., 2020; Li et al., 2019). Facing the massive MS data, the post-acquisition data processing is necessary to screen the metabolites of interest, and mass defect filtering (MDF) (An et al., 2021), neutral loss filtering (NLF) (Luo et al., 2019), and fragment filtering (Gao et al., 2017), *etc.*, have been reported for this purpose. Impressively, the joint application of MS^n acquisition, neutral loss scanning (NL), precursor ion scanning (PRE), and selective reaction monitoring (SRM), rendering a "compound to extract to formulation" strategy, was developed, by which 131 metabolites were identified from the biofluids of rats after administration of the TCM formula Gegen-Qinlian Decoction (Qiao et al., 2016).

Aimed to comprehensively identify the drug metabolites covering more trace components, in this work, we presented an integral strategy by combining PIL-DDA and $HDMS^E$/MDF on two LC-MS platforms (QTrap 4500 and Vion^{TM} IM-QTOF). It was validated by characterizing the metabolites of DHC from diverse rat tissues (e.g., plasma, bile, urine, and feces), and the general technical routine was exhibited in Fig. 1. Theoretical metabolites of DHC were largely predicted to generate a PIL based on the known biotransformation pathways. Two DDA approaches containing the created PIL were developed using multiple ion monitoring-information dependent acquisition-enhanced product ions scan (MIM-IDA-EPI) on QTrap 4500 and high-definition DDA (HDDDA) on Vion IM-QTOF, which were both coupled with ultra-high performance liquid chromatography (UHPLC). Moreover, a DIA approach using $HDMS^E$ on Vion IM-QTOF was established, and MDF was utilized for the data processing to target the metabolites of interest. The superiority of the integrated strategy, established in the current work, over the conventional approaches were discussed, as well.

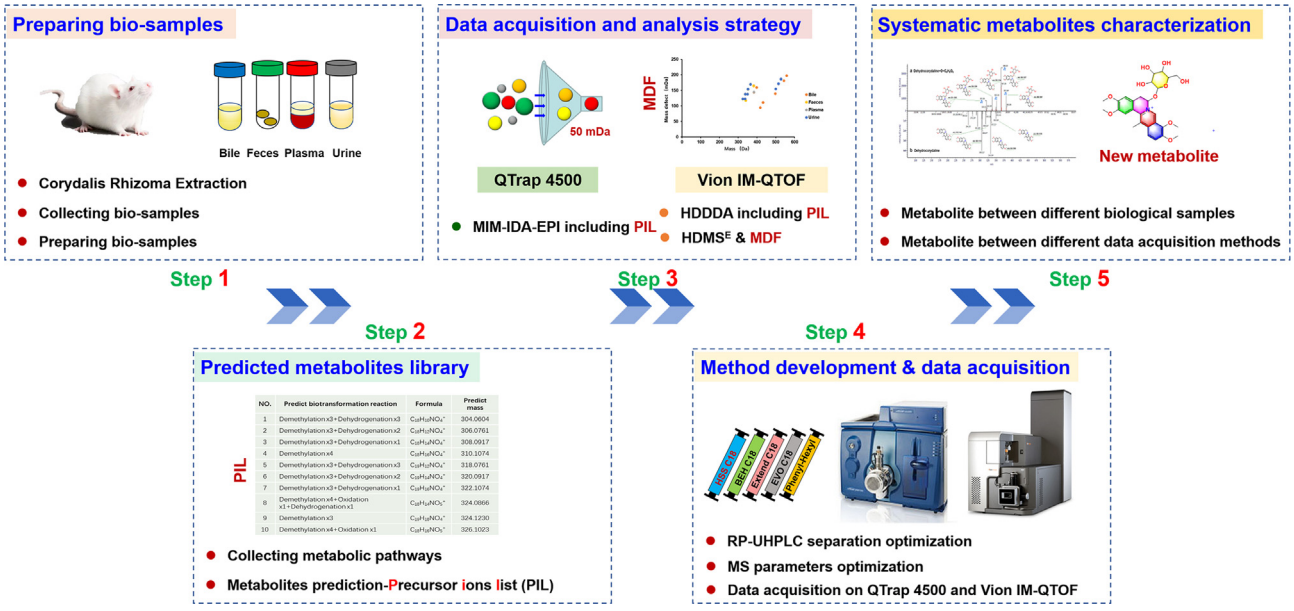

Fig. 1 The analytical strategy for identifying the metabolites of DHC from diverse rat tissue samples by precursor ions list-including DDA and HDMS^E on two LC-MS platforms (QTrap 4500 and IM-QTOF).

2. Experimental

2.1. Chemicals and reagents

Dehydrocorydaline (DHC), was prepared from the dried tuber of *C. yanhusuo* in our laboratory, and the structure was established by the ^{1}H NMR and ^{13}C NMR analyses (Table S1; Figs. S1–S3). The purity of DHC was above 95.0% determined by HPLC-UV (at 280 nm). Acetonitrile (ACN), methanol (MeOH), and formic acid (FA) of the LC-MS grade, were purchased from Fisher Scientific (Fisher, Fair Lawn, NJ, USA). Deionized water (18.2 MΩ·cm at 25℃) was prepared by a Milli-Q Integral 5 water purification system (Millipore, Bedford, MA, USA).

2.2. Animals

Animal experiments were performed using the male Sprague-Dawley (SD) rats (220–250 g; animal license No.1100112011021709), which were purchased from Beijing Vital River Laboratory (Beijing, China). The rats were kept in an environmentally controlled breeding room with temperature at 25 ± 2℃, relative humidity at 55 ± 10%, and 12 h light/12 h dark cycle. Before the experimentation, all rats were fed and watered freely for a week. Then rats were kept in the metabolic cages and were fasted over the night but with free access to water before the test. Urine, feces, and plasma, were collected before the oral administration of DHC (100 mg/kg, in 0.5% CMC-Na aqueous solution) as the control and after DHC administration during the time intervals of 0–8, 8–24, and 24–48 h. Rats were given free access to the food and water after oral administration for 3 h. Blood (1 mL) was collected at each time from the ophthalmic veins and centrifuged (1,699 g) at 4℃ for 10 min to separate the supernatant. After the 7-day recovery, the rats were anesthetized with 10% (*w*/*v*) chloral hydrate solution (3.0 mL/kg) by the intraperitoneal injection, and bile duct intubation was performed. Bile sample was collected before and after an oral dose administration of DHC (100 mg/kg, in 0.5% CMC-Na aqueous solution), individually regarded as the control group and the experimental group. The experimental group bile samples were collected during the time intervals of 0–4, 4–8, and 8–24 h. All samples were immediately frozen at − 80 ℃ until the analysis.

This study was carried out in accordance with the guidelines established by the Association for Assessment and Accreditation of Laboratory Animal Care. All experimental procedures were approved by the Animal Care and Use Committee of the Tianjin University of Traditional Chinese Medicine (protocol No. TJAB-TJU20200032).

2.3. Sample preparation

All the samples were thawed at room temperature. Plasma (50 μL), bile (50 μL), urine (500 μL), and feces (100 mg) at each time point, were separately mixed together equally. The homogeneous biosamples from different rats were merged into a collective sample. Then, samples were vortex-mixed for 3 min after the addition with three-fold volume of MeOH in the polypropylene test tube. Feces was porphyrized by sonication for 15 min. Then the plasma, bile, urine, and feces, were centrifuged (1,699 g) at 4℃ for 10 min to remove the precipitated protein. The supernatant fractions were transferred to another polypropylene test tube and evaporated under the steady flow of N_2. The residues were re-dissolved in 150 μL of MeOH. The samples were centrifuged at 20,817 g and 4℃ for 10 min, with the supernatant taken as the test solution.

2.4. UHPLC/QTrap-MS and UHPLC/IM-QTOF-MS

Chromatographic separation of diverse rat biosamples was performed on the Waters Acquity UPLC I-Class system (Waters, Milford, MA, USA) consisting of a binary solvent

system, an online degasser, an autosampler, and a thermostatically column controller. The sample separation was carried out on a Waters HSS C18 SB (2.1 × 100 mm, 1.8 μm) column at 30℃ using the mobile phase consisting of solvent A (0.1% FA in water) and solvent B (ACN). An optimized gradient elution was used as follows: 0–7 min, 10%–30% B; 7–15 min, 30%–45% B; 15–18 min, 45%–60% B; 18–21 min, 60%–65% B; 21–29 min, 65%–75% B; 29–32 min, 75%–80% B; and 32–35 min, 80%–95% B. The flow rate was set at 0.3 mL/min, and the injection volume for each biosample was set at 2 μL.

The MS data for characterizing the metabolites of DHC were recorded on two LC-MS platforms: QTrap 4500 (AB Sciex Scientific, Concord, Canada) and Vion™ IM-QTOF (Waters, Milford, MA, USA). Both two mass spectrometers were equipped with the electrospray ionization (ESI) source and recorded the MS data across the range of *m*/*z* 100–1500 in the positive mode. The operating parameters of QTrap 4500 were optimized as follows: curtain gas, 35 psi; ion source gas 1 and gas 2, 45 psi; ionspray voltage, 5500 V; temperature, 550℃; declustering potential, 80 V; collision energy, 50 eV and spread of 10 eV; scan rate of linear ion trap, 4000 amu/s. A LockSpray ion source on Vion IM-QTOF was equipped using the following parameters: capillary voltage, 1.0 kV; cone voltage, 100 V; source offset, 80 V; desolvation gas temperature, 500℃; source temperature, 120℃; desolvation gas flow (N_2), 800 L/h; and cone gas flow (N_2), 50 L/h. The travelling wave IM separation was conducted under the default parameters, and CCS calibration was consistent with the manufacture′s guidelines using a mixture of calibrants (Paglia et al., 2015). Detailed information for the settings in all MS scan approaches is depicted below. Analyst 1.7.0 software (AB Sciex Scientific, Concord, Canada) and Waters UNIFI 1.9.3.0 software (Waters, Milford, MA, USA) were separately utilized to control the MS data collection by QTrap 4500 and Vion IM-QTOF, respectively.

2.5. PIL-DDA and HDMS^E

Both PIL-DDA and HDMS^E were employed to recorded the collision-induced dissociation MS^2 (CID-MS^2) information for DHC metabolites. The metabolites of DHC were predicted to create the PIL. Given that DHC belongs to the proberberine-type alkaloid, all metabolic pathways ever-reported about the proberberine alkaloids were collected in the first step. In detail, the following criteria were employed: 1) the known metabolic pathways reported for DHC, probeberine-type alkaloid (such as panamatinine) and *C. yanhusuo* in rat tissues (Table S2); 2) all metabolic pathways in the Met ID of the UNIFI software (Table S3); 3) the limit for the metabolic pathway, and up to 4 for the demethylation transformation. Based on these considerations, the PIL was created (Table S4).

PIL-DDA was set on QTrap 4500 using MIM-IDA-EPI and Vion IM-QTOF using HDDDA. For the IDA criteria on QTrap 4500, when the signal intensity of the selected ion was greater than 100,000 (threshold), the EPI scans of the three most abundant precursor ions were triggered at the collision energy of 30–50 eV. For HDDDA of the QTOF mass analyzer, the mass analyzer scanned at a low energy of 6 eV and at 0.3 s per scan (MS^1), and mass-dependent ramp collision energy (MDRCE) set at 30 eV for low mass and 50 eV for high mass. When TIC (total ion chromatogram) intensity exceeded 200 detector counts, the MS/MS fragmentation of three most intense precursors was automatically triggered at 0.2 s per scan over a mass range of *m*/*z* 100–1500. For HDMS^E on Vion IM-QTOF, ramp collision energy of 30–50 eV was set for the high-energy fragmentation at 0.3 s per scan.

2.6. Automatic peak annotation of the high-resolution PIL-DDA and HDMS^E data

The raw data obtained by HDDDA and HDMS^E were corrected by the UNIFI software (Waters) with the reference at *m*/*z* 556.276575, the mass tolerance less than 10 ppm, and the signal-to-noise ratio threshold greater than 3. All peaks with MS ion intensity greater than 1500.0 counts and MS/MS ion intensity greater than 600.0 counts, were extracted. The processed HDDDA data were analyzed manually for characterizing DHC metabolites. The corrected HDMS^E data were processed by the computational intelligent metabolic response prediction combined with 50 mDa of MDF to track the possible metabolites. Moreover, automatic matching of the product ions (*m*/*z* 350.1387, 334.1074, 318.1125, 308.1281, and 306.1125) and the neutral loss forms (CH_3, SO_3, and $C_6H_8O_6$) was set, which could assist to efficiently screen the metabolites of interest.

In addition, the raw data obtained by MIM-IDA-EPI on QTrap 4500 were processed by the Analyst software (AB Sciex Scientific) and manually analyzed for characterizing the structures of DHC metabolites.

3. Results and discussion

3.1. The integral strategy for the in-depth drug metabolites characterization

Identification of the drug metabolites from biosamples by LC-MS is often encountered with severe interference from the endogenous substances. Conventional data acquisition by DDA always records very limited number of the useful MS^n data related to the drug metabolites because of their low concentration in the biosamples. It thus becomes crucial to develop more potent analytical strategy to separate and identify more drug metabolites at the trace amount.

Previous practice in comprehensively characterizing the herbal metabolites can demonstrate the addition of PIL containing the precursor ions in DDA enables the simultaneous targeted/untargeted metabolites characterization both on the Q Exactive Q-Orbitrap and Vion IM-QTOF mass spectrometers (Fu et al., 2019; Wang et al., 2021a). In this mode, the targeted precursor ions recorded in the MS^1 spectrum were endowed with the highest priority to automatedly trigger the MS^2 fragmentation. Additionally, DIA, by MS^E/HDMS^E or SWATH, can in theory record the MS^2 data of all precursor ions, and therefore greatly benefit the discovery of drug metabolites (Kang et al., 2020; Radchenko et al., 2020). In the aspect of the mass spectrometers, the QTrap series, by the linear connection of quadrupole (Q) and ion trap (IT) mass analyzers, can enable the simultaneous substructure or neutral loss-based survey scan and EPI scan by IDA (Li et al., 2019; Song et al., 2018). These IDA approaches are particularly

for the untargeted characterization of the complex metabolites. In addition, the application of IM-MS in metabolites characterization can enable the additional dimension of separation of the gas-phase ions generating high-definition MS spectra, and more importantly, offers the CCS values useful for the isomers differentiation (Wang et al., 2020; Wang et al., 2021a; Wang et al., 2022). It is noted that automatic peak annotation workflows have been well established on the Vion IM-QTOF mass spectrometer to process the MS^E, DDA, $HDMS^E$, and HDDDA data (Jia et al., 2019; Liu et al., 2022; Wang et al., 2021a; Wang et al., 2022; Zhang, et al., 2019).

These considerations prompt us to formulate an integral strategy by combining PIL-DDA and DIA on two mass spectrometers (QTrap 4500 and Vion IM-QTOF) to comprehensively characterize the drug metabolites, using DHC as a case (Fig. 1). It involves the biosample preparation, PIL construction, method development/data acquisition, and the systematic metabolites characterization.

3.2. Metabolites prediction to create the precursor ions list

The main metabolic pathways of DHC *in vivo* have been known to involve *O*-demethylation, hydroxylation, di-hydroxylation, glucuronidation of *O*-demethyl DHC, sulfation of *O*-demethyl DHC and di-hydroxylation of dehydro-DHC (Guan et al., 2017). Thus, we carried out the molecular design for DHC metabolites based on the molecular structure characteristics and the known primary metabolic products. The following cases are considered. Firstly, DHC has four methoxy groups attached to C-2/C-3 on ring A and C-9/C-10 on ring D, which may suffer from demethylation to render new hydroxyl groups easily conjugated with glucuronic acid and sulfinic acid. Secondly, the C-5 and C-6 sites on ring B are adjacent to the sp^2-hybrid carbon atom in the C ring, which are prone to ω-oxidation. Thirdly, the C-8 site on ring C and the C-11/C-12 sites on the D ring are located in the *ortho-* or *para-*position of the electron substituent on the aromatic ring, which may undergo hydroxylation and oxidation. Fourthly, the introduced new hydroxyl groups are prone to sulfuration and glucuronidation. As a result, a table containing 419 theoretical metabolites for DHC was generated (Table S4), which was included in the MIM-IDA-EPI (QTrap 4500) and HDDDA (Vion IM-QTOF) scan approaches, respectively.

3.3. Optimization of the RP-UHPLC and MS conditions

As the efforts in the first step, the stationary phase was screened by using acetonitrile (ACN) and 0.1% FA in H_2O as the mobile phase. We had compared five sub 2-μm particles packed chromatographic columns from Waters, Agilent, and Phenomenex, by detecting the parent drug of DHC dissolved in methanol, which involved BEH C18, Kinetex EVO C18 (2.1 × 100 mm, 1.7 μm), HSS C18 SB, Zorbax Extend C18 (2.1 × 100 mm, 1.8 μm), and CSH Phenyl-Hexyl (2.1 × 100 m m, 1.7 μm). The results showed that, compared with the others, HSS C18 SB enabled stronger retention of DHC with very high column efficiency (Fig. 2a). The HSS C18 SB particles can well retain the basic compounds using the acidic mobile phase (pH: 2.0–8.0).

With the view of achieving highly sensitive detection of DHC and its metabolites, the key ESI source parameters in the positive ion mode of QTrap 4500 and Vion IM-QTOF were optimized by comparing the peak area of DHC precursor ion as the indicator. On the QTrap 4500 mass spectrometer, single-factor experiments were employed to sequentially optimize the ionspray voltage (3500–5500 V), source temperature (450–500℃), and declustering potential (DP, 60–140 V). It was observed that the increase in ionspray voltage and source temperature within the tested variation ranges generally positively correlated with the response of DHC, and the maximum peak area values were enabled at 5500 V of ionspray voltage and 500℃ of source temperature, respectively. But different trend was observed by adjusting DP, as the low level (at 60 V) could induce ions to cluster, and the higher setting (100–140 V) could cause the in-source fragmentation. Therefore, DP of 80 V was regarded as the best choice (Fig. 2b). Similarly, the influences of capillary voltage (1000–3000 V) and cone voltage (20–100 V) on Vion IM-QTOF were assessed. We found the response of DHC negatively and positively correlated to the increasing of capillary voltage and cone voltage, respectively (Fig. 2c). Impressively, the precursor ion of DHC almost disappeared at capillary voltage of 3000 V. Accordingly, the capillary voltage at 1000 V and the cone voltage at 100 V were finally selected.

3.4. Comprehensive characterization of the metabolites from the plasma, bile, urine, and feces of rats after oral administration of DHC

The parent drug of DHC could be easily identified by comparing with the reference compound by the characteristics of retention time (16.16 min) and MS^1/MS^2 information. Interestingly, the $[M-e]^+$ molecular ions were observed for DHC both on QTrap 4500 and IM-QTOF because of its property of being a quaternary ammonium alkaloid (Du et al., 2018). According to the MS/MS spectrum obtained by the high-resolution Vion IM-QTOF, the characteristic fragments of DHC were detected at *m/z* 350.1357 $[M-CH_4]^+$, 336.1177 $[M-2CH_3]^+$, 334.1063 $[M-2CH_4]^+$, 322.1429 $[M-CH_4-CO]^+$, 308.1267 $[M-2CH_3-CO]^+$, and 306.1113 $[M-2CH_4-CO]^+$ (Fig. 3).

The CID-MS^2 spectra of the rat tissue samples (e.g., bile, plasma, urine, and feces) were interpreted in the similar manner for structural elucidation of DHC metabolites. Consequently, a total of 40 metabolites of DHC were characterized from four rat bio-samples, with the results of QTrap 4500 listed in Table S5 and those recorded by IM-QTOF in Table S6, respectively. In summary, the identification workflows could involve two steps. Firstly, through the binary comparison of the MS data for the bile, feces, plasma, and urine samples recorded before and after the drug administration, all credible metabolites signals were screened out. Secondly, the characteristic fragments for the prototype of DHC and the unknown metabolites were comparatively analyzed for the structural identification. Taking **M40** (t_R = 11.66 min, *m/z* 558.1972) detected in the drug-administrated bile sample as an example, its molecular formula was induced as $C_{28}H_{32}NO_{11}$ (mass error: 0.4 ppm). The MS/MS spectrum showed a product ion of *m/z* 382.1641 by eliminating 176 Da, indicating the neutral elimination of $C_6H_8O_6$ (Fig. 4). Interestingly, a series of characteristic fragments were observed, such as *m/z* 382.1641, 366.1328, 352.1164, 338.1328,

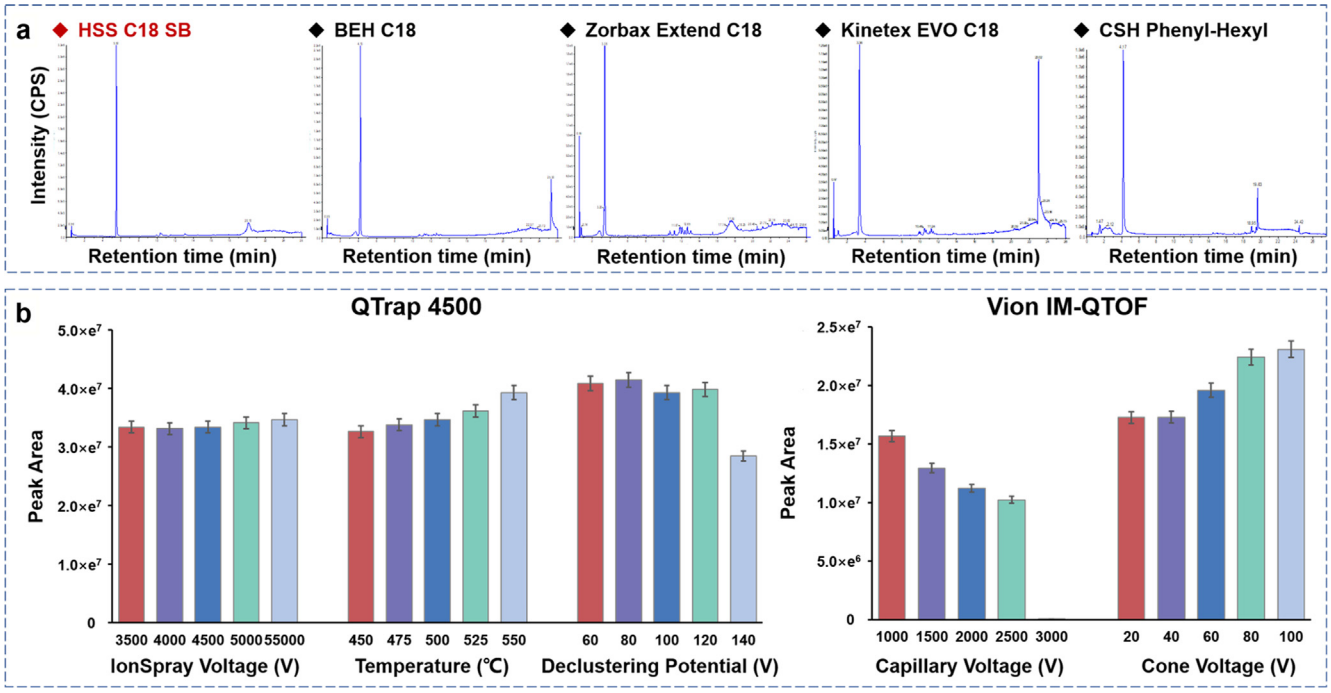

Fig. 2 Method development for establishing the UHPLC-MS approaches: (a) selection of stationary phase for the reversed-phase UHPLC separation of DHC; (b) optimization of key parameters of the QTrap 4500 and Vion IM-QTOF mass spectrometers for detecting DHC in the positive ESI mode ($n = 3$).

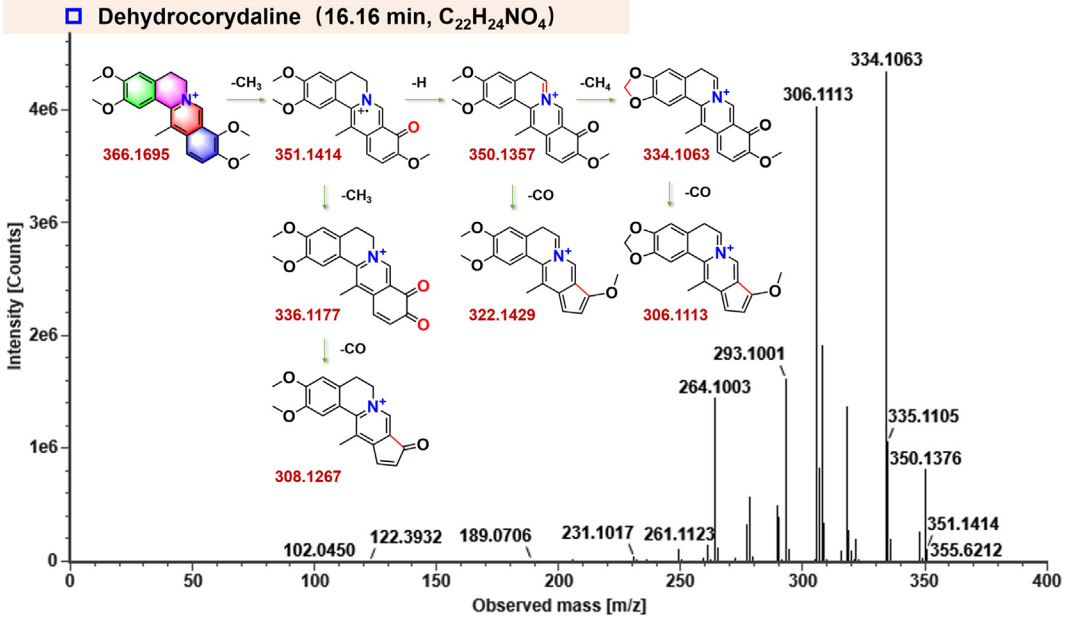

Fig. 3 The proposed fragmentation pathways for DHC.

and 321.1352. It was thus inferred as an oxidation-glucuronidation metabolite of DHC.

Multiple metabolic pathways were identified in rat tissues after oral administration of DHC. First, phase Ⅰ metabolic reactions could occur for multiple times, such as the products of double demethylation reactions (**M6**, **M7**, and **M8**), triple demethylation (**M1**, **M2**, and **M3**), and double oxidation (**M22**, **M23**, and **M24**), which displayed the mass shifts of –28 Da, –32 Da, and + 32 Da, compared with the parent drug of DHC, respectively. Second, the metabolites suffering from different types of phase Ⅰ metabolic reactions were identified, such as the metabolites of the demethylation and the double oxidation reactions (**M20** and **M21**), the demethylation and the dehydrogenation reactions (**M10**), the triple demethylation and the oxidation reaction (**M9**), the triple demethylation and double oxidation reactions (**M15**), the double demethylation

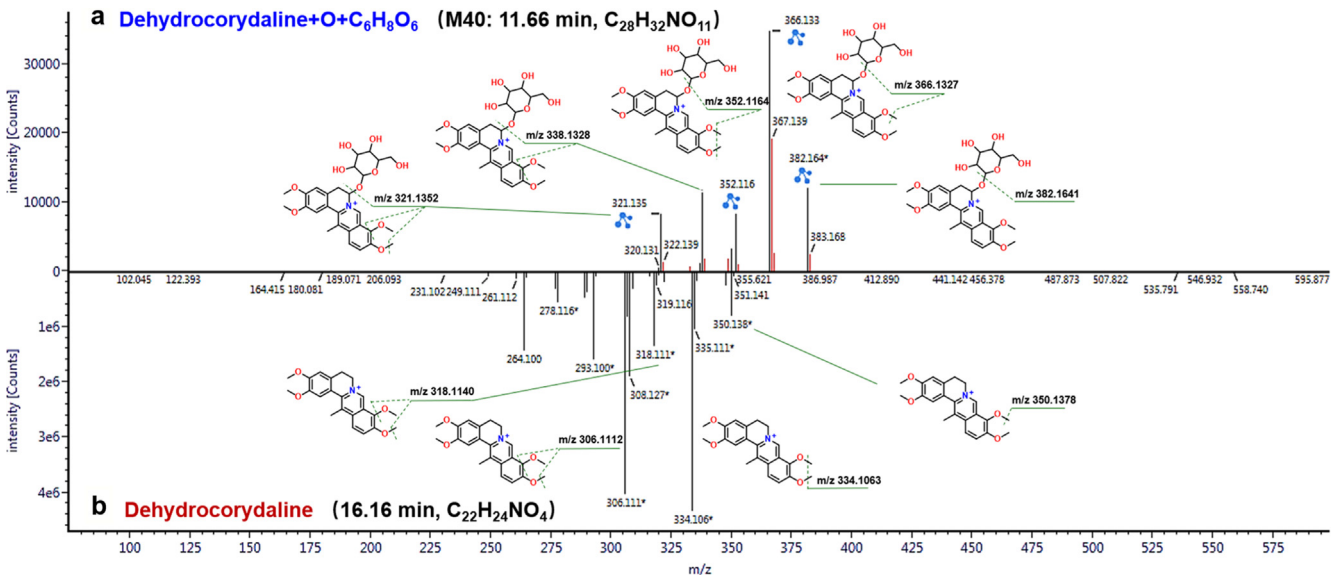

Fig. 4 Comparison of the MS/MS spectra between DHC and one of the metabolites (**M40**, oxidation and glucuronidation metabolite) to illustrate its characterization.

and the double oxidation reactions (**M16** and **M17**), together with the double demethylation and the dehydrogenation reactions (**M4** and **M5**). Third, the phase Ⅱ metabolic reactions occurred after the demethylation reaction or the oxidation reaction on DHC, the MS^2 spectra of which exhibited the characteristic transitions of $[M-SO_3]^+$ and $[M-C_6H_8O_6]^+$ by neutral loss of 80 Da and 176 Da, respectively.

The presence of multiple isomeric metabolites demonstrated the differentiated biotransformation sites on DHC, even if they were characterized with the similar metabolic routes. They gave different retention time and differential CCS values (Tables S5 and S6). We have outlined the metabolic pathways of DHC in rats, as presented in Fig. 5. The involved four methoxy groups and positions 5-/6-/8- on the skeleton were the main metabolic sites. Additionally, DHC also underwent demethylation and oxidative metabolism, followed by further biotransformation of glucuronic acid conjugation and sulfuric acid conjugation. Compared with the literature (Guan et al., 2017), the metabolites of DHC in the urine and feces of rats were newly reported, while 16 biotransformation pathways were found for the first time,and 17 new metabolites were identified in bile.

3.5. Comparison of DHC metabolites in different rat tissue samples and the performance of different data acquisition strategies

The metabolites characterized from different tissues (bile, plasma, urine, and feces) were compared to probe the potential metabolic difference (Fig. 6). In detail, 30 from bile (**M1**, **M3**, **M4**–**M6**, **M7**, **M10**–**M14**, **M17**–**M20**, **M22**, **M23**, **M25**–**M29**, **M32**, **M33**, **M35**–**M40**), 16 from feces (**M2**–**M10**, **M12**–**M14**, **M16**, **M18**, **M19**, **M24**), 7 from plasma (**M2**, **M6**, **M14**, **M21**, **M35**, **M37**, **M38**), and 18 from urine (**M3**–**M8**, **M10**, **M12**–**M15**, **M30**, **M32**–**M37**), got characterized (Tables S5 and S6; Fig. 6c). The most diverse metabolites were detected in bile, and the fewest in plasma. As previously reported, the prototype berberine drug could be rapidly eliminated from the blood and was excreted through bile in rats, resulting in lower blood concentration in the body (Zuo et al., 2006). A Venn diagram was ploted to visualize the metabolites overlapping from these four biosamples (Fig. 6a), and there were many metabolic pathways occurring to different tissues. For instance, two metabolites, **M14** and **M16**, were characterized from four biological samples. Meanwhile, different metabolites present in different number of tissue samples were summarized (Fig. 6b).

Totally three MS experiments (MIM-IDA-EPI including PIL, HDDDA including PIL, and $HDMS^E$) on two mass spectrometers (QTrap 4500 and IM-QTOF) were employed to identify the metabolites of DHC. Notably, combination of the DDA and DIA approaches enabled the discovery of more minor metabolites. For example, on the same instrument of IM-QTOF, HDDDA missed the characterization of **M4**, **M25**, and **M9**, in comparison with the $HDMS^E$. It demonstrated DIA-MDF was a powerful strategy in drug metabolites characterization. Additionally, most of the predicted metabolites failed to be detected, which indicated the restricted biotransformation or low concentration of diverse metabolites in the biosamples. The total ion chromatograms collected by different mass spectrometers and MS methods are displayed in Fig. S4.

4. Conclusion

In the present study, we integrated PIL-DDA and DIA-MDF to establish the analytical platform aimed to detect the metabolites of DHC in rat plasma, urine, bile, and feces, after oral administration. In total, 40 metabolites were tentatively identified from four biological samples, and the metabolic pathways of DHC in rats were proposed as well. There were significant differences in the types and quantities of the metabolites in these four biosamples. The combination of DDA and DIA could extend the coverage and ensure the high

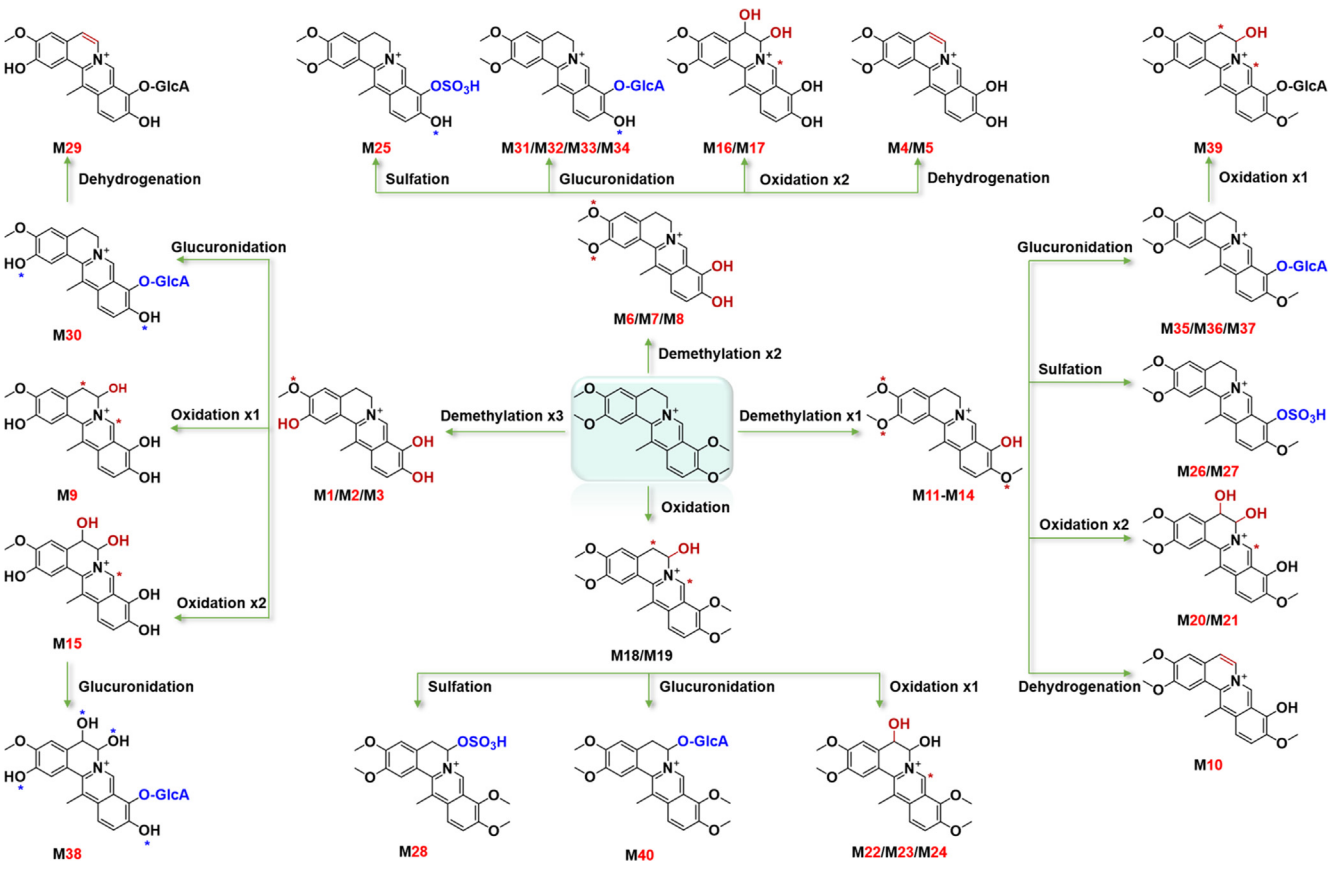

Fig. 5 The proposed metabolic pathways for DHC in different tissues of rats.

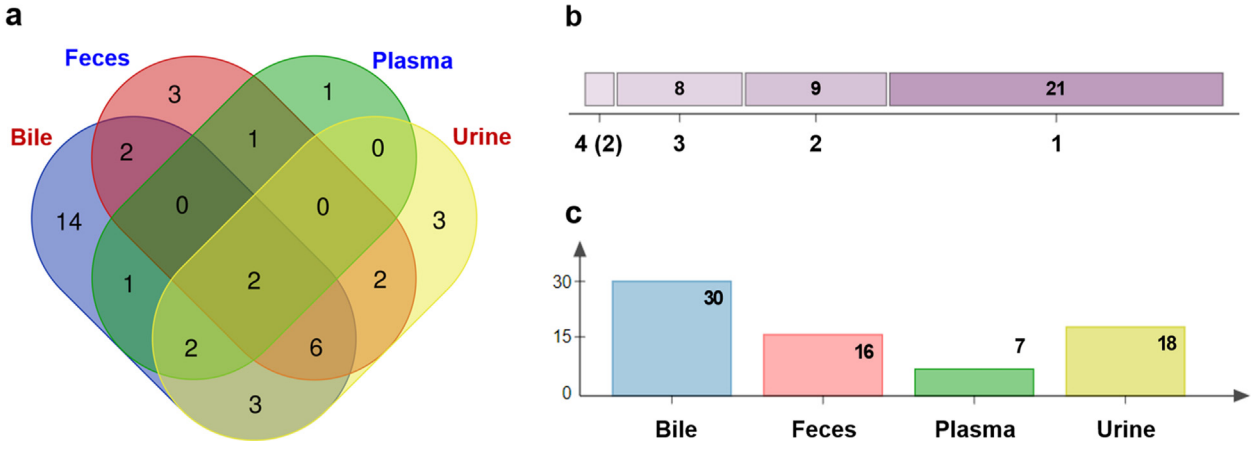

Fig. 6 Summary on the metabolites characterization results of DHC. (a) Ven diagrams of the overlapping metabolites in each biosample; (b) the common and specific metabolites among plasma, bile, urine, and feces; (c) the number of metabolites identified in plasma, bile, urine, and feces.

quality of MS spectra. DIA coupled with MDF is a powerful strategy for the comprehensive drug metabolites characterization, with high degree of automation and high analysis efficiency. Additionally, the CCS value derived from IM separation was provided on Vion IM-QTOF, and its role in characterizing isomeric metabolites deserves further investigation. To our knowledge, the *in vivo* metabolism of DHC in rat urine and feces is reported for the first time, and the metabolites characterized from bile are much more than the previous reports, which can testify the feasibility and potency of the developed approaches in the characterization of drug metabolites.

The authors declared that there is no conflict of interest.

Declaration of Competing Interest

The authors declare that they have no known competing financial interests or personal relationships that could have appeared to influence the work reported in this paper.

Acknowledgements

This work was financially supported by National Natural Science Foundation of China (Grant No. 81872996) and Natural Science Foundation of Tianjin of China (Grant No. 20JCYBJC00060).

Appendix A. Supplementary material

Supplementary data to this article can be found online at https://doi.org/10.1016/j.arabjc.2022.103968.

References

An, Y. L., Wei, W. L., Li, H. J., Li, Z. W. Yao, C. L., Qu, H., Yao, S., Huang, Y., Zhang J. Q., Bi, Q. R., Li, J. T., Guo, D. A., 2021. An enhanced strategy integrating offline superimposed two-dimensional separation with mass defect filter and diagnostic ion filter: comprehensive characterization of steroid alkaloids in Fritillariae Pallidiflorae Bulbus as a case study. J. Chromatogr A. 1643, 462029. https://doi.org/ 10.1016/j.chroma.2021.462029.

Chen, Y.C., Li, C., Yi, Y.D., Du, W.J., Jiang, H.J., Zeng, S., Zhou, H., 2020. Organic cation transporter 1 and 3 contribute to the high accumulation of dehydrocorydaline in the heart. Drug Metab. Dispos. 48, 1074–1083. https://doi.org/10.1124/DMD.120.000025.

Dong, F., Wang, S.P., Yang, A.L., Li, Q.Y., Wang, Y.Q., Dai, L., Tao, Y.F., Wei, X., Zhang, J.Y., 2020. Systematic screening and characterization of cardamonin metabolites using UHPLC-Q-Exactive Orbitrap MS after oral administration to rats. Arab. J. Chem. 13, 8768–8782. https://doi.org/10.1016/j.arabjc.2020.10.007.

Du, W.J., Jin, L.S., Li, L.P., Wang, W., Zeng, S., Jiang, H.D., Zhou, H., 2018. Development and validation of a HPLC-ESI-MS/MS method for simultaneous quantification of fourteen alkaloids in mouse plasma after oral administration of the extract of *Corydalis yanhusuo* Tuber: application to pharmacokinetic study. Molecules 23, 714. https://doi.org/10.3390/molecules23040714.

Fu, L.L., Ding, H., Han, L.F., Jia, L., Yang, W.Z., Zhang, C.X., Hu, Y., Zuo, T.T., Gao, X.M., Guo, D.A., 2019. Simultaneously targeted and untargeted multicomponent characterization of Erzhi Pill by offline two-dimensional liquid chromatography/quadrupole-Orbitrap mass spectrometry. J. Chromatogr. A 1584, 87–96. https://doi.org/10.1016/j.chroma.2018.11.024.

Gao, X., Mu, J.Q., Li, Q., Guan, S.Y., Liu, R., Du, Y.Y., Zhang, H. F., Bi, K.S., 2017. Comprehensive identification of Guan-Xin-Shu-Tong capsule via a mass defect and fragment filtering approach by high resolution mass spectrometry: *in vitro* and *in vivo* study. Molecules 22, 1007. https://doi.org/10.3390/molecules22061007.

Guan, H.Y., Li, K.T., Wang, X.M., Luo, X.M., Su, M.F., Tan, W.T., Chang, X.Y., Shi, Y., 2017. Identification of metabolites of the cardioprotective alkaloid dehydrocorydaline in rat plasma and bile by liquid chromatography coupled with triple quadrupole linear ion trap mass spectrometry. Molecules 22, 1686. https://doi.org/10.3390/molecules22101686.

Hu, G.R., Dong, Z., Wang, X.X., Bai, L.C., Lei, Q., Yang, J., Li, L., Li, Q., Liu, L.C., Zhang, Y.L., Ji, Y.C., Guo, L.Y., Liu, Y.L., Cui, R.J., 2019. Dehydrocorydaline inhibits cell proliferation, migration and invasion via suppressing MEK1/2-ERK1/2 cascade in melanoma. OncoTargets Ther. 12, 5163–5175. https://doi.org/10.2147/OTT.S183558.

Jia, L., Zuo, T.T., Zhang, C.X., Li, W.W., Wang, H.D., Hu, Y., Wang, X.Y., Qian, Y.X., Yang, W.Z., Yu, H.S., 2019. Simultaneous profiling and holistic comparison of the metabolomes among the flower buds of *Panax ginseng*, *Panax quinquefolius*, and *Panax notoginseng* by UHPLC/IM-QTOF-HDMS^E-based metabolomics analysis. Molecules 24, 2188. https://doi.org/10.3390/molecules24112188.

Jin, L.S., Zhou, S.S., Zhu, S.J., Lei, S.W., Du, W.J., Jiang, H.D., Zeng, S., Zhou, H., 2019. Dehydrocorydaline induced antidepressant-like effect in a chronic unpredictable mild stress mouse model via inhibiting uptake-2 monoamine transporters. Eur. J. Pharmacol. 864,. https://doi.org/10.1016/j.ejphar.2019.172725 172725.

Kang, D., Ding, Q.Q., Xu, Y.F., Yin, X.X., Guo, H.M., Yu, T.J., Wang, H., Xu, W.S., Wang, G.J., Liang, Y., 2020. Comparative analysis of constitutes and metabolites for traditional Chinese medicine using IDA and SWATH data acquisition modes on LC-Q-TOF MS. J. Pharm. Anal. 10, 588–596. https://doi.org/10.1016/j.jpha.2019.11.005.

Kong, X.P., Chen, Z.C., Xia, Y.J., Liu, E.L., Ren, H.Q., Wang, C., Hu, W.H., Dong, T.X., Pi, R.B., Tsim Karl, W.K., Cuman Roberto, K.N., 2020. Dehydrocorydaline accounts the majority of anti-Inflammatory property of Corydalis Rhizoma in cultured macrophage. Evid-Based Compl. Alt. 2020, 4181696. https://doi.org/10.1155/2020/4181696.

Li, M.R., Si, D.D., Fu, Z.F., Sang, M.M., Zhang, Z.X., Liu, E.W., Yang, W.Z., Gao, X.M., Han, L.F., 2019. Enhanced identification of the *in vivo* metabolites of Ecliptae Herba in rat plasma by integrating untargeted data-dependent MS^2 and predictive multiple reaction monitoring-information dependent acquisition-enhanced product ion scan. J. Chromatogr. B 1109, 99–111. https://doi.org/10.1016/j.jchromb.2019.02.001.

Li, Q.Y., Li, K.T., Sun, H., Jin, W., Shi, J.W., Shi, Y., 2014. LC-MS/MS determination and pharmacokinetic study of dehydrocorydaline in rat plasma after oral administration of dehydrocorydaline and *Corydalis yanhusuo* extract. Molecules 19, 16312–16326. https://doi.org/10.3390/molecules191016312.

Li, H.J., Wei, W.L., Li, Z.W., Wang, M.Y., Wei, X.M., Cheng, M.Z., Yao, C.L., Bi, Q.R., Zhang, J.Q., Li, J.Y., Guo, D.A., 2021. An enhanced strategy integrating offline two-dimensional separation with data independent acquisition mode and deconvolution: Characterization of metabolites of *Uncaria rhynchophylla* in rat plasma as a case. J. Chromatogr. B 1181, 122917 https://doi.org/10.1016/j.jchromb.2021.122917.

Liu, J., Wang, H.D., Yang, F.F., Chen, B.X., Li, X., Huang, Q.X., Li, J., Li, X.Y., Li, Z., Yu, H.S., Guo, D.A., Yang, W.Z., 2022. Multi-level fingerprinting and cardiomyocyte protection evaluation for comparing polysaccharides from six *Panax* herbal medicines. Carbohydr. Polym. 277,. https://doi.org/10.1016/j.carbpol.2021.118867 118867.

Luo, K.W., Xing, Y.D., 2021. Identification strategies of Chinese materia medica and complex prescription metabolites *in vivo*. J. Gansu Univ. Chin. Med. 38 (1), 91–96.

Luo, Y., Lai, C. J. S., Zhang, J., Feng, Y. L., Wen, Q., Tan, T., 2019. Comprehensive metabolic profile of phenolic acids and flavonoids in Glechomae Herba using ultra-high-performance liquid chromatography coupled to quadrupole-time-of-flight tandem mass spectrometry with diagnostic ion filtering strategy. J. Pharm. Biomed. Anal. 164, 615–629. https:/doi.org/10.1016/j.jpba.2018.11.017.

Paglia, G., Angel, P., Williams, J.P., Richardson, K., Olivos, H.J., Thompson, J.W., Menikarachchi, L., Lai, S., Walsh, C., Moseley, A., Plumb, R.S., Grant, D.F., Palsson, B.O., Langridge, J., Geromanos, S., Astarita, G., 2015. Ion mobility-derived collision cross section as an additional measure for lipid fingerprinting and identification. Anal. Chem. 87, 1137–1144. https://doi.org/10.1021/ac503715v.

Qiao, X., Wang, Q., Wang, S., Miao, W.J., Li, Y.J., Xiang, C., Guo, D.A., Ye, M., 2016. Compound to extract to formulation: a

knowledge-transmitting approach for metabolites identification of Gegen Qinlian Decoction, a traditional Chinese medicine formula. Sci. Rep. 6, 39534. https://doi.org/10.1038/srep39534.

Radchenko, T., Kochansky, C.J., Cancilla, M., Wrona, M.D., Mortishire-Smith, R.J., Kirk, J., Murray, G., Fontaine, F., Zamora, I., 2020. Metabolite identification using an ion mobility enhanced data-independent acquisition strategy and automated data processing. Rapid Commun. Mass Spectrom. 34,. https://doi.org/10.1002/rcm.8792 e8792.

Song, Q.Q., Liu, W.J., Chen, X.J., Li, J., Li, P., Yang, F.Q., Wang, Y. T., Song, Y.L., Tu, P.F., 2018. Serially coupled reversed phase-hydrophilic interaction liquid chromatography-tailored multiple reaction monitoring, a fit-for-purpose tool for large-scale targeted metabolomics of medicinal bile. Anal. Chim. Acta 1037, 119–129. https://doi.org/10.1016/j.aca.2017.11.072.

Wang, H., Bi, F.J., Lin, T., Jiang, Y.Q., 2017a. RP-HPLC fingerprint of *Corydalis yanhusuo* and content determination of nine alkaloids. J. Chin. Med. Mater. 40 (3), 624–629.

Wang, H.D., Wang, H.M., Wang, X.Y., Xu, X.Y., Hu, Y., Li, X., Shi, X.J., Wang, S.M., Liu, J., Qian, Y.X., Gao, X.M., Yang, W.Z., Guo, D.A., 2022. A novel hybrid scan approach enabling the ion-mobility separation and the alternate data -dependent and data-independent acquisitions (HDDIDDA): Its combination with off-line two-dimensional liquid chromatography for comprehensively characterizing the multicomponents from Compound Danshen Dripping Pill. Anal. Chim. Acta 1193, 339320. https://doi.org/10.1016/j.aca.2021.339320.

Wang, H.D., Wang, S.M., Zhao, D.X., Xie, H.M., Wang, H.M., Sun, M.X., Yang, X.N., Qian, Y.X., Wang, X.Y., Li, X., Gao, X.M., Yang, W.Z., 2021a. A novel ion mobility separation-enabled and precursor ions list-included high-definition data-dependent acquisition (HDDDA) approach: Method development and its application to the comprehensive multicomponent characterization of Fangji Huangqi Decoction. Arab. J. Chem. 14, 103087. https://doi.org/10.1016/j.arabjc.2021.103087.

Wang, L. E., Zhang, Y., Wang, Z. W., Gong, N., Kweon, T. D., Vo, B., Wang, C. R., Zhang, X. L., Chung, J. Y., Alachkar1, A., Liang, X. M., Luo, D. L., Civelli1, O., 2016. The antinociceptive properties of the *Corydalis yanhusuo* extract. PLoS One 11, e0162875. https://doi.org/10.1371/journal.pone.0162875.

Wang, S.M., Qian, Y.X., Sun, M.X., Jia, L., Hu, Y., Li, X., Wang, H. D., Huo, J.H., Wang, W.M., Yang, W.Z., 2020. Holistic quality evaluation of Saposhnikoviae Radix (Saposhnikovia divaricata) by reversed-phase ultra-high performance liquid chromatography and hydrophilic interaction chromatography coupled with ion mobility quadrupole time-of-flight mass spectrometry-based untargeted metabolomics. Arab. J. Chem. 13, 8835–8847. https://doi.org/10.1016/j.arabjc.2020.10.013.

Xiao, W.P., Yang, Y.F., Wu, H.Z., Xiong, Y.Y., 2019. Predicting the mechanism of the analgesic property of yanhusuo based on network pharmacology. Nat. Prod. Commun. 14 (10). https://doi.org/10.1177/1934578X19883071.

Yu, C.J., Wang, F.Y., Liu, X.Y., Miao, J.Y., Tang, S.Q., Jiang, Q., Tang, X.D., Gao, X.Y., 2021. Corydalis Rhizoma as a model for herb-derived trace metabolites exploration: A cross-mapping strategy involving multiple doses and samples. J. Pharm. Anal. 11, 308–319. https://doi.org/10.1016/j.jpha.2020.03.006.

Yu, Y., Yao, C.L., Guo, D.A., 2021. Insight into chemical basis of traditional Chinese medicine based on the state-of-the-art techniques of liquid chromatography-mass spectrometry. Acta Pharm. Sin. B 11 (6), 1469–1492. https://doi.org/10.1016/j.apsb.2021.02.017.

Zhang, A.H., Sun, H., Yan, G.L., Wang, X.J., 2017. Recent developments and emerging trends of mass spectrometry for herbal ingredients analysis. Trends Anal. Chem. 94, 70–76. https://doi.org/10.1016/j.trac.2017.07.007.

Zhang, C.X., Zuo, T.T., Wang, X.Y., Wang, H.D., Hu, Y., Li, Z., Li, W.W., Jia, L., Qian, Y.X., Yang, W.Z., Yu, H.S., 2019. Integration of data-dependent acquisition (DDA) and data-independent high-definition MS^E ($HDMS^E$) for the comprehensive profiling and characterization of multicomponents from *Panax japonicus* by UHPLC/IM-QTOF-MS. Molecules 24, 2708. https://doi.org/10.3390/molecules24152708.

Zhang, Y.P., Wang, Z.H., Xu, J., Yang, F.F., Dai, C.F., Xie, W.J., Liang, Z., Su, S.B., 2020. Optimization of the extraction and purification of *Corydalis yanhusuo* W.T. Wang based on the Q-marker uniform design method. BMC Chem. 14, 9. https://doi.org/10.1186/s13065-020-00666-6.

Zuo, F., Nakamura, N., Akao, T., Hattori, M., 2006. Pharmacokinetics of berberine and its main metabolites in conventional and pseudo germ-free rats determined by liquid chromatography/ion trap mass spectrometry. Drug Metab. Dispos. 34, 2064–2072. https://doi.org/10.1124/dmd.106.011361.